

Reversible evanescent wave sensors for hydrazine

Michael T. Carter*, Jimmy R. Smith, Donald R. Mowry and Jay G. Patel

Eltron Research, Inc.
5660 Airport Blvd., Suite 105
Boulder, CO 80301-2340

ABSTRACT

We report recent progress on development of evanescent wave fiber optic sensors for hydrazine (HZ), monomethylhydrazine (MMH) and unsymmetrical dimethylhydrazine (UDMH). Chemically reversible evanescent sensors capable of detection below 10 ppb were prepared by removing cladding from commercial multimode fiber and coating the exposed core with a hydrazine-sensitive triphenylmethane dye immobilized in an inert polymer matrix, typically poly(vinylchloride). Triphenylmethane dyes bleach reversibly in the presence of hydrazines, enabling colorimetric sensing. The linear dynamic range was typically 0 - 300 ppb and overall dynamic range up to *ca.* 5 ppm. Sensors optimized for HZ were as much as a factor of 45 less sensitive to MMH and UDMH, suggesting that the sensor film would require optimization for each analyte. Saturation response and relaxation times were on the order of 5 - 8 min, but measurable signals for 10 ppb HZ could be obtained in under 30 s. These sensors demonstrate a novel route to reversible sensing of these highly toxic compounds.

Keywords: fiber optic sensor, reversible, hydrazine, UDMH, hypergolic fuel, evanescent wave

1. INTRODUCTION

Neat liquid hydrazines including hydrazine (HZ), monomethylhydrazine (MMH) and unsymmetrical dimethylhydrazine (UDMH), shown in Figure 1, are used as hypergolic fuels in aerospace applications. Aerozine 50, a 50:50 v/o mixture of HZ and UDMH is one common fuel formulation used by the Air Force. Hydrazine propellants are employed in satellites and manned spacecraft by NASA. Hydrazine is also used widely as an oxygen scavenging anticorrosive agent by the electric power industry and in the synthesis of drugs, fertilizers and polymers¹. Exposure to hydrazines can have carcinogenic, teratogenic, immunotoxic and neurotoxic effects². As a consequence of the many serious health hazards of these materials, very low exposure limits are recommended. The American Conference of Government Industrial Hygienists (ACGIH), for example, has recently recommended a threshold limit value (TLV) of 10 ppb over an eight hour day or a dosimetric 80 ppb-hr. Transient levels not to exceed 50 ppb for any 15 min interval will necessitate real-time, reversible sensing.

The widespread presence of hydrazine in aerospace applications has prompted much work on devices for low-level detection. Recently reported methods of detection for gas phase hydrazines have included chemiluminescence³, electrochemistry⁴, ion mobility mass spectrometry⁵, photoionization⁶ and chemiresistors based on irreversible conductivity changes in a conductive polymer⁷. The reversible fiber optic sensing approach reported here is intended to compliment these other technologies and to address some needs for low level HZ detection which have not been previously fulfilled. Chemical sensors based on fiber optic technology could be particularly advantageous for hydrazine sensing in the aerospace arena because they present no spark hazard and are readily adaptable to remote placement or deployment in arrays. They can therefore be used safely in areas where large amounts of combustible materials are stored and can be used to continuously monitor wide areas^{8,9}.

Fiber optic sensors have been shown promising for measurement of gas phase hydrocarbons and chlorinated hydrocarbons by IR spectroscopy¹⁰⁻¹⁴. The analytes are very nonpolar and therefore partition well into the polysiloxane cladding of the optical fiber where they are detected by characteristic IR absorptions. Colorimetric halocarbon optical fiber

*Corresponding author. Email: mtcarter@EltronResearch.com; phone: 303/440-8008; fax: 303/440-8007

probes are also possible in other configurations¹⁵. Fiber optic dosimeters and dosimeter arrays based on colorimetric chemistry between hydrazine and phosphomolybdic acid^{16,17} have been reported and are complimentary to our reversible sensor. We intended to show that a simple, yet sensitive true chemical sensor for hydrazines could be achieved based on an evanescent wave configuration.

2. EXPERIMENTAL

2.1 Reagents.

Malachite green carbinol hydrochloride (Sigma-Aldrich) was dissolved in water which was subsequently evaporated to give the free triphenylmethane dye (malachite green, MG) by intramolecular dehydration of the carbinol. Low molecular weight polyvinylchloride (PVC), tetrahydrofuran (THF) and PVC plasticizer (bis-(2-ethylhexyl) sebacate, BEHS) were from Sigma-Aldrich and used as received. Hydrazine, ammonia, water, sulfur dioxide and methylamine were generated from permeation tubes obtained from KinTek, Inc. (La Marque, TX). The generator/dilution system for delivery of continuously variable hydrazine concentrations to the sensor is described below.

2.2 Sensor Preparation.

Fiber optic sensors were prepared using commercially available, multimode, polymer-coated silica optical fiber from General Fiber Optics. The silica core, polysiloxane cladding and nylon jacket thicknesses were 1000 μm , 50 μm and 50 μm , respectively. The refractive indices of the core (n_1) and cladding (n_2) were 1.458 and 1.400, respectively. Cladding was removed from 2 cm in the middle of a 10 cm section of fiber to expose the silica core. Dynasolve 210 (Dynalloy Corp., Hanover, NJ) was used to dissolve remaining cladding after initial mechanical removal with a razor blade. The exposed core was rinsed with high purity water and dried in air.

Exposed cores were coated with a thin layer of PVC containing plasticizer and MG, denoted PVC-MG. Films were cast by dip-coating the core in a tetrahydrofuran (5 mL) solution containing 0.5 weight percent (w/o) MG, 28.5 w/o PVC and 71 w/o BEHS. These values represent an empirically determined optimum formulation of the coating solution for HZ detection. This formulation was used in all experiments unless indicated otherwise. Physical manipulations required to prepare the sensor necessitated using a large fiber core diameter to maintain a suitable degree of mechanical strength once the cladding was removed. The once-dipped fiber was allowed to dry in air, in the dark prior to use.

2.3 Measurements.

The experimental system for generation of hydrazine vapor, dilution with carrier gas and delivery of the diluted mixture to the fiber optic sensor is shown schematically in Figure 2. The permeation tube temperature was usually controlled at 25 °C, which gave a flux of *ca.* 8×10^{-5} mg HZ/min. Nitrogen was passed through the generator at a constant flow rate (100 mL/min), then mixed downstream with diluent nitrogen at a variable flow rate of 0 - 2500 mL/min. Higher HZ concentrations were obtained by heating the permeation tube to increase analyte flux. After passing through the sensor compartment, effluent was passed through a bubbler containing 0.1 M H_2SO_4 to quantitatively trap HZ. Contents of the trap were analyzed using a commercially available colorimetric analyzer (Hydraver, Hach, Inc. Loveland, CO) to determine average flux of the permeation tube over the course of an experiment, typically once each day. We manually determined flux rate of our tubes because actual emission rates deviated substantially from manufacturer specifications. The permeation tubes were very sensitive to changes in experimental conditions and required several days to equilibrate following variations of, e.g., carrier gas flow rate or temperature.

Interferent studies using methylamine (CH_3NH_2), ammonia (NH_3), water (H_2O) and sulfur dioxide (SO_2) involved adding a controlled flux of interferent to the flow system. Kintek tubes as described above for CH_3NH_2 , NH_3 and SO_2 were assumed to flux at the nominal rates provided by the manufacturer. Moisture addition was monitored using a commercially available humidity sensor (Ohmic Instruments HC-600) installed in the test system. Moisture saturation was achieved by bubbling dry N_2 gas into water through a dispersion tube before entering the test cell.

Sensors were interrogated in two ways. For experiments where spectral information was desired, a tungsten-halogen light source was coupled into the sensor and evanescent wave absorption characteristics were examined with an Ocean Optics

(Dunedin, FL) SD-2000 UV-Visible spectrometer. The light source and spectrometer are fully compatible with standard fiber optic couplers and optical components. Spectral data were acquired using Ocean Optics SpectraScope software. For sensor experiments requiring only a generic detector response as a function of time, the sensor was illuminated with a 3 mW, 635 nm diode laser (Sanyo DL-3038-051) operated in CW mode. Changes in transmitted power during HZ exposure were monitoring with a Burr-Brown (OPT-209) PIN photodiode detector-amplifier combination, the output of which was acquired on a laboratory computer using locally written software. The experimental apparatus is shown in Figure 3. All experiments were performed in a fume hood. The test system components were mounted on a small optical bench (Edmund Scientific). All experiments were performed at the ambient temperature of the laboratory, 22° - 27° C.

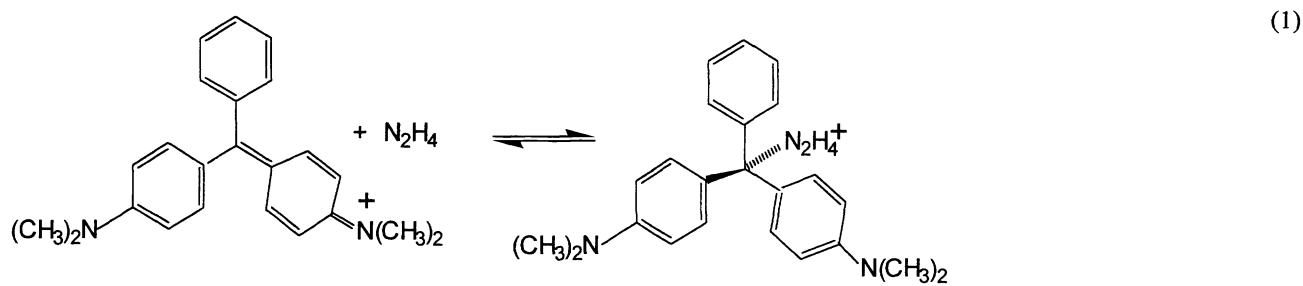
3. RESULTS AND DISCUSSION

3.1 Optical Fiber Modification.

A schematic diagram of the evanescent wave sensor is shown in Figure 4. The polymer coating, low molecular weight PVC, was smooth and continuous, as observed by SEM, over the entire cylindrical area where the original polysiloxane cladding had been removed. Under typical coating conditions, PVC films were 5 - 30 μm thick. Coating thicknesses were estimated by examination of SEM cross-sections. Although our coating method did not give highly controlled film thicknesses, response times and other sensor characteristics were comparable between sensors. Attempts to improve coating thickness control included using a stepper motor to reproducibly withdraw the fiber from the coating solution and vapor phase priming of the exposed core with hexamethyldisilazane prior to coating to improve wettability to THF. These attempts failed to improved coating control.

3.2 Triphenylmethane Dye Chemistry.

In the presence of hydrazines, malachite green (MG) and other triphenylmethane dyes bleach rapidly and reversibly^{18,19}:



The free triphenylmethane dye exhibits a strong visible absorption band centered at 621 nm²⁰, whereas the adduct formed by reversible interaction of N₂H₄ with the acidic central triphenylmethane carbon atom is colorless. This chemistry has several important consequences. First, the reversible reaction allows true sensing rather than dosimetry. Second, the transition from an intensely colored species in the absence of analyte to a colorless one in the presence of analyte allows sensitive measurements since analyte detection is manifested as an increase in transmitted optical power. Chemistry between HZ and MG can proceed in the absence of solvent, simplifying the sensor configuration.

Evanescent wave power decays exponentially away from the core-cladding interface according to⁸:

$$I(z) = I_0 \exp(-z/d_p) \quad (2)$$

where $I(z)$ and I_0 are evanescent wave power at distance z and at the core-cladding interface, respectively and d_p is given by

$$d_p = (\lambda/4\pi) [(n_1^2 \sin^2 \theta - n_2^2)]^{-1/2} \quad (3)$$

where λ is the wavelength of incident light, θ is the incident angle and n_1 and n_2 are the refractive indices of the core and cladding (the PVC/MG film), respectively. Exponential decay of the evanescent field with distance into the cladding limits chemical sensing interactions to within about $ca.$ one wavelength of the core-cladding interface. The fraction of total transmitted power carried by the evanescent wave increases with decreasing fiber diameter. It would therefore be advantageous to use smaller fiber diameters for these sensors, since the evanescent wave is not used to full advantage in large diameter fiber. Wider diameter cores, however, give greater mechanical strength which is needed in this configuration.

Transmission UV-visible spectra for HZ bleaching of MG are shown in Figure 5. These spectra are qualitatively similar to conventional UV-visible transmission experiments. Bleaching corresponds to an increase in transmitted light intensity which is the basis of the analytical measurement. Classical absorption during interaction with MG, where internal reflection of light propagating in the PVC film occurs at the air-PVC interface, cannot be ruled out. Quantitative evaluation of this is difficult presently since the refractive index of the PVC film is not known.

Spectral resolution of sensor response is generally not required. We performed most experiments with a PIN photodiode detector whose raw output was the analytical signal. Typical results are shown in Figures 6 and 7. Figure 6 shows raw, unfiltered sensor response to a high HZ concentration, 5.4 ppm. Figure 7A shows a typical low-level raw sensor response to 10 ppb HZ. Differences in measurement sensitivity, as reflected by the relative magnitudes of the photodiode response at high and low HZ exposures, reflect incremental improvements in signal-to-noise ratio achieved during this work. Reversibility of the bleaching chemistry of Eqn. (1) is clear in these experiments. The PVC matrix did not respond significantly to HZ exposure in the absence of MG, although HZ permeability into PVC is required to elicit a response. All sensors showed some degree of baseline slope which is evident in Figures 6 and 7. While the source is not certain, it cannot be attributed to instrumental drift or temperature fluctuations, but may be caused by irreversible photobleaching of MG or irreversible reductive degradation of MG by HZ.

3.3 Sensor Response.

Typical low level concentration dependence of the sensor is shown in Figure 7B. The dynamic range of the sensor exceeded 0 - 2 ppm HZ. In experiments with MMH, not shown, nonlinear dynamic ranges up to 6 ppm were observed for the same sensor configuration, with significantly attenuated sensitivity. The HZ linear dynamic range was $ca.$ 0 - 300 ppb. At extremely low HZ concentrations, as in Figure 7B, linear response was observed with a lower limit of detection (LLD) 0.4 ± 0.1 ppb, based on $\pm 3\sigma$ of the noise and the average sensitivity of a set of five sensors.

Sensor response was characterized in terms of rise time to span 10% to 90% of saturation and relaxation from 90% to 10% of baseline after achieving saturation, denoted $t_{10/90}$ and $t_{90/10}$, respectively. Sensor response to 10 ppb HZ was commonly $5 \text{ min} \leq t_{10/90}, t_{90/10} \leq 8 \text{ min}$ when the sensor continuously resided within the test chamber of Figure 2. When the sensor was allowed to relax to baseline by physically removing it from the test chamber, baseline was regained in $ca.$ 10% of the time required otherwise. These results suggested that the apparent response of the sensor was a convolution of the real response time by the PVC-MG film and a second time constant derived from the experimental apparatus. The surface activity of HZ and resulting complications in analytical measurements are well known^{1,5}. Therefore, it is likely that the overall response time exhibited a significant contribution from slow adsorption and desorption of HZ at the interior walls or dissolution into the tubing of the delivery system. Nonetheless, the minimum time needed to obtain a signal significantly above noise for 10 ppb HZ was ≤ 30 s, suggesting that real-time field monitoring can be realized with this sensor.

3.4 Interferences.

Responses to several potential interferences, including NH_3 , SO_2 , CH_3NH_2 and H_2O were investigated. NH_3 and CH_3NH_2 were chosen to examine effects of chemically similar basic gases which could display similar chemistry. SO_2 was chosen as a representative acidic analyte, which was not expected to elicit a response. H_2O was used to test relative humidity variations on sensor response.

The effect of moisture on the MG absorption spectrum, taken on-fiber, is shown in Figure 8. On-fiber transmission UV-Vis spectra of MG were examined under dry nitrogen and water-saturated nitrogen atmospheres. The absorption envelope of MG was unaffected by moisture, but the baseline shifted to larger absorbance values, corresponding to a decrease in transmitted power relative to a dry film. This is consistent with swelling of the PVC film on uptake of water vapor²¹. Variation of relative

humidity was not deleterious to sensor performance. Figure 9 shows an experiment in which 5.4 ppb HZ was detected, with a slight *increase* in sensitivity, after a step in relative humidity from 0 to 64 %. In a series of measurements over a range of relative humidities spanning 10 % to 75 %, the overall effect was a slight enhancement (*ca.* 3%) in sensitivity with increasing relative humidity. This may result from enhanced diffusion of HZ within the swollen PVC film. The PVC film responded rapidly and reversibly to step changes in humidity at relative humidities of 50 - 100 %. However, since instantaneous changes in relative humidity are not common in the field, it is not likely that the ability to detect HZ will be compromised by this behavior. Sensor response to humidity could be compensated in a field system, for example, by simultaneous measurement of relative humidity and selection of an appropriate calibration curve for HZ concentration under those conditions.

NH₃ interference was investigated over a range of ratios of HZ:NH₃ spanning excess HZ to excess NH₃. Figure 10 shows results at 1:1 HZ:NH₃ ratio. The selectivity ratio for HZ over NH₃ varied from 2.2 to 230 depending on the magnitude of HZ and NH₃ concentrations. For example, the selectivity ratio was 2.2 at a HZ:NH₃ ratio of 1:1 where 8.3 ppb and 8.4 ppb NH₃ were used, but rose to 6.7 at HZ: NH₃ =1:1 with HZ and NH₃ concentrations of 62 and 66 ppb (Fig. 10). This was probably a reflection of differences in HZ and NH₃ sensitivities with increasing concentrations. The selectivity was 230 for 53 ppb HZ and 1 ppm NH₃, showing that HZ selectivity was greatest at the highest NH₃ concentrations.

CH₃NH₂ showed HZ:CH₃NH₂ selectivities of 2.8 to 14 depending on the concentration of CH₃NH₂. Higher interferent concentrations yielded higher selectivities, again the likely result of more extreme sensitivity loss for the interferent at higher concentrations. Sulfur dioxide, SO₂, an acidic interferent, could not be detected with our sensor, even at concentrations as high as 1 ppm. This probably was due to inability of SO₂ to bleach MG and is consistent with the proposed mechanism of chemical sensing^{18,19}.

4. CONCLUSIONS

Reversible evanescent wave fiber optic sensors were prepared using a thin coating of poly(vinylchloride) containing malachite green, to detect hydrazine at concentrations ≤ 10 ppb in the gas phase. These sensors, to our knowledge, represent the first example of reversible, gas phase detection of hydrazines. Reversible bleaching of dye in the presence of hydrazine enabled extremely sensitive measurements, with a lower limit of detection of *ca.* 0.4 ppb and performance well suited to ACGIH guidelines. Sensors were responsive to other basic gases such as ammonia. Further work will be needed to improve selectivity to HZ. Modulation of permeability properties of the PVC film may be possible by varying the plasticizing agent or polymer matrix used to cast sensor films.

5. ACKNOWLEDGMENTS

This work was supported via Small Business Innovation Research Grants F29601-96-C-0024 and F29601-95-C-0128 from The United States Air Force Phillips Laboratory, Kirtland AFB, Albuquerque, NM with technical oversight from USAF Space and Missile Systems Center, Los Angeles AFB, CA.

6. REFERENCES

1. E. W. Schmidt, *Hydrazine and its derivatives*, pp. 713 - 856, Wiley, New York, 1984.
2. R. Von Burg and T. Stout, "Toxicology update: hydrazine", *J. Appl. Toxicol.* **11** (6), pp. 447 - 450, 1991.
3. G. E. Collins, S. Latturmer and S. L. Rose-Pehrsson, "Chemiluminescence detection of hydrazine vapor", *Talanta* **42** (4), pp. 543 - 555, 1995.
4. J. R. Stetter, K. A. Tellefsen, R. A. Saunders and J. J. DeCorpo, "Electrochemical Determination of Hydrazine and Methyl- and 1,1-Dimethylhydrazine in Air", *Talanta* **26**, pp. 799 - 804, 1979.
5. G. A. Eiceman, M. R. Salazar, M. Rodriguez, T. F. Limero, S. W. Beck, J. H. Cross, R. Young, and J. T. James, "Ion mobility spectrometry of hydrazine, monomethylhydrazine and ammonia in air with 5-nonanone reagent gas", *Anal. Chem.* **65** (13), pp. 1696 - 1702, 1993.
6. J. R. Stetter, C.-X. Shi and G. J. Maclay, "Modulated photoionization detection of hydrazine compounds in mixtures without prior separation", *Anal. Chem.* **63** (17), pp. 1755 - 1759, 1991.
7. D. L. Ellis, M. R. Zakin, L. S. Bernstein and M. F. Rubner, "Conductive polymer films as ultrasensitive chemical sensors

- for hydrazine and monomethylhydrazine vapor", *Anal. Chem.* **68** (5), pp. 817 - 822, 1996.
8. W. R. Seitz, "Chemical sensors based on immobilized indicators and fiber optics", *CRC Crit. Rev. Anal. Chem.* **19**(2), pp. 135 - 173, 1988 .
 9. O. Wolfbeis, "Gas Sensors", *Fiber Optic Chemical Sensors and Biosensors*, O. S. Wolfbeis (Ed.), **I**, pp. 55 - 81, CRC Press, Boca Raton, 1991.
 10. D. S. Blair, L. W. Burgess and A. M. Brodsky, "Study of analyte diffusion into a silicone-clad fiber-optic chemical sensor by evanescent wave spectroscopy", *Appl. Spectrosc.* **49** (11), pp. 1636 - 1645, 1995.
 11. B. Mizaikoff, K. Taga and R. Kellner, "Infrared fiber optic gas sensor for chlorofluorocarbons", *Vibr. Spectrosc.* **8**, pp. 103 - 108, 1995.
 12. J.-P. Conzen, J. Burck and H.-J. Ache, "Characterization of a fiber-optic evanescent wave absorbance sensor for nonpolar organic compounds", *Appl. Spectrosc.* **47** (6), pp. 753 - 763, 1993.
 13. E. F. Carome, G. Fischer and V. Kubulins, "Fiber-optic sensor system for hydrocarbon vapors", *Sens. Actuators B* **13-14**, pp. 305 - 308, 1993.
 14. F. P. Milanovich, S. B. Brown, B. W. Colston, P. F. Daley and K. C. Langry, " A fiber-optic sensor system for monitoring chlorinated hydrocarbon pollutants", *Talanta* **41** (12), pp. 2189 - 2194, 1994.
 15. S. M Klainer, K. Goswami, D. K. Dandge, S. J. Simon, N. R. Herron, D. Eastwood and L. A. Eccles, "Environmental monitoring applications of fiber optic chemical sensors (focs), *Fiber optic chemical sensors and biosensors*, O. S. Wolfbeis (Ed.), **II**, pp. 83 -122, CRC Press, Boca Raton, 1991.
 16. C. Klimcak, G. Radhakrishnan and B. Jadaszliwer, "A remote fiber optic dosimeter network for detecting hydrazine vapor", *Optical sensors for environmental and chemical process monitoring*, I. D. Aggarwal, S. Farquharson and E. Koglin (Eds.), **2367**, pp. 80 - 88, SPIE, Bellingham, WA, 1995.
 17. C. Klimcak, G. Radhakrishnan, S. Delcamp, Y. Chan, B. Jadaszliwer and S. Moss, "Development of a fiber optic chemical dosimeter network for use in the remote detection of hydrazine propellant vapor leaks at cape canaveral air force station", *Chemical, biochemical and environmental fiber sensors VI*, R. A. Lieberman (Ed.), **2293**, pp. 209 - 219, SPIE, Bellingham, WA, 1994.
 18. A. T. Vartanyan, "The reversible bleaching of solid layers of triphenylmethane dyes in hydrazine vapor", *Russ. J. Phys. Chem.* **35** (10), pp. 1105 - 1109, 1961.
 19. A. T. Vartanyan, "A spectroscopic investigation of interaction between hydrazine and neutral dyes with phenolic hydroxy-groups", *Russ. J. Phys. Chem.* **36** (10), pp. 1142-1145, 1962.
 20. N. R. Ayyangar and B. D. Tilak, "Basic Dyes", *The chemistry of synthetic dyes*, K. Venkataraman (Ed.), **IV**, pp. 103 - 159, Academic press, New York, 1971.
 21. D. J. Harrison, X. Li and S. Petrovic, "Water and the ion-selective electrode membrane", *Biosensors and chemical sensors*, P. G. Edelman and J. Wang (Eds.), **487**, pp. 292 - 300, The American Chemical Society, Washington, 1992.

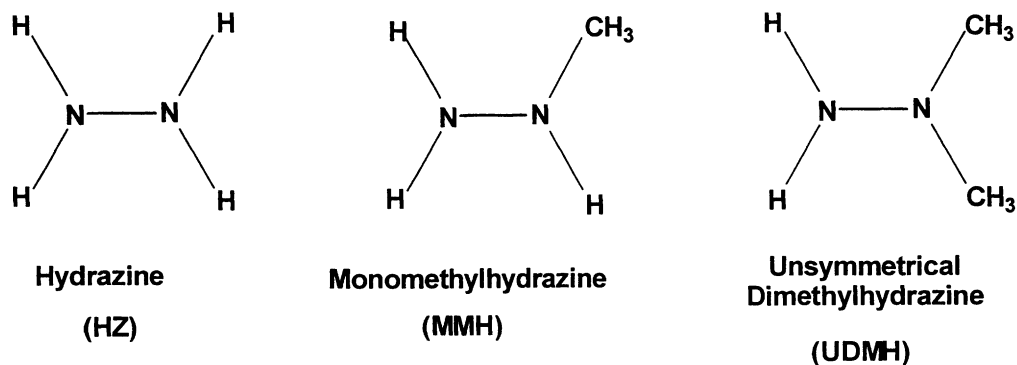


Figure 1. Chemical structures of common hydrazines.

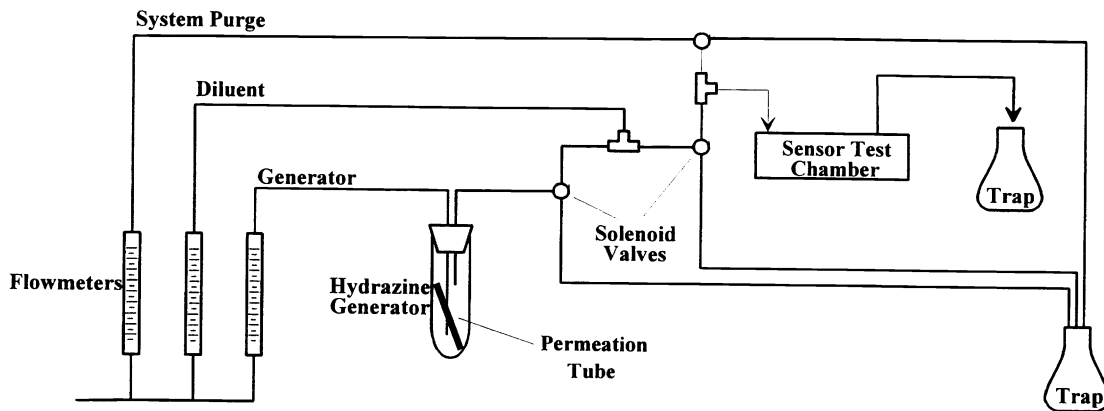


Figure 2. Hydrazine generator, gas dilution and delivery system.

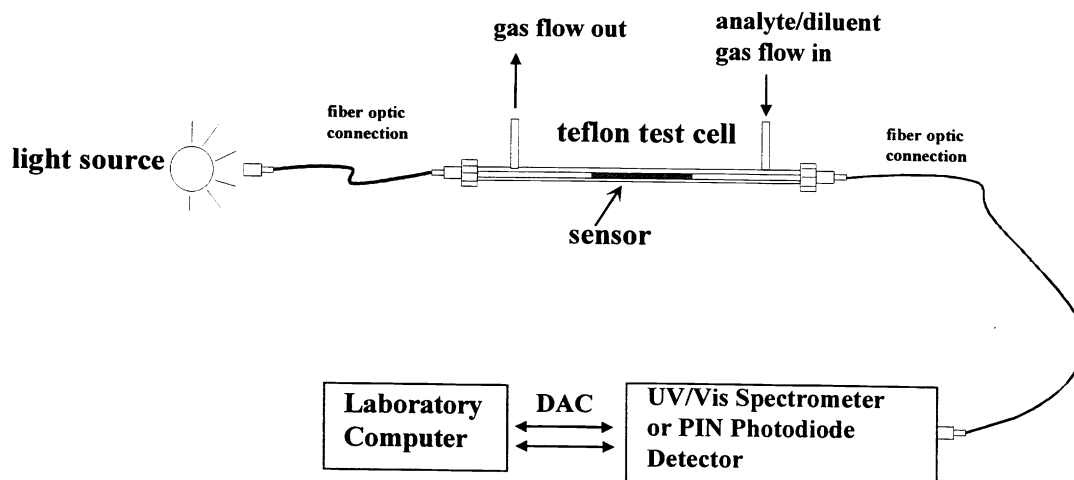


Figure 3. Experimental arrangement for fiber optic sensor interrogation.

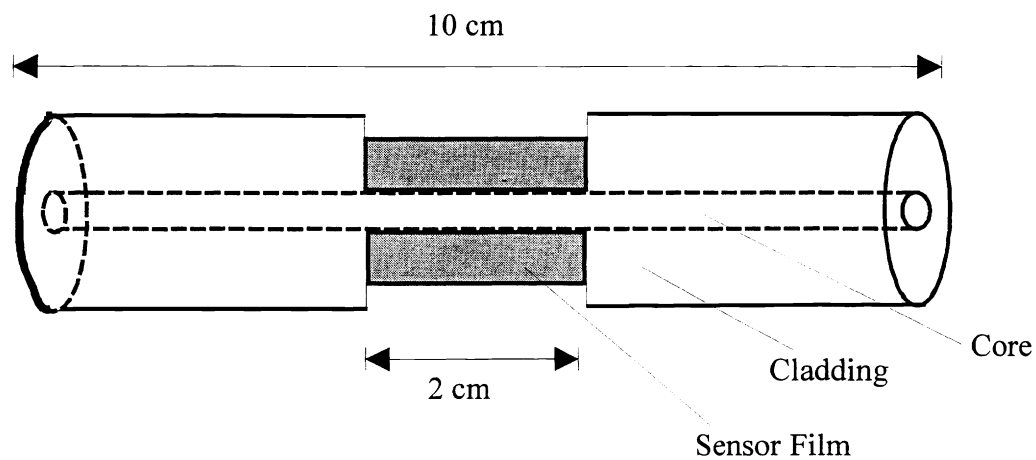


Figure 4. Layout of the fiber optic hydrazine sensor.

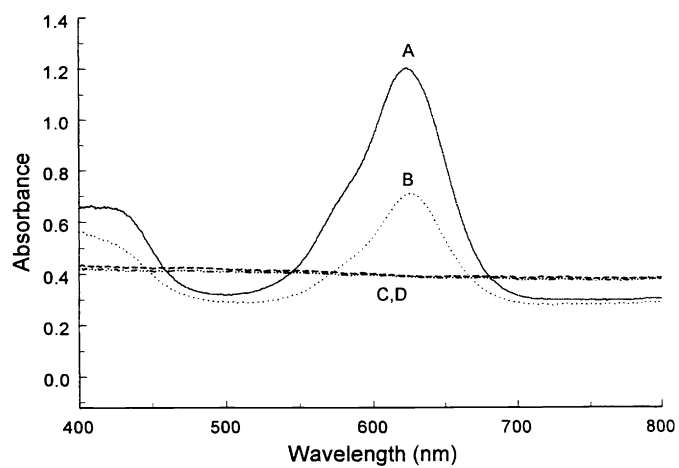


Figure 5. On-fiber UV-visible absorption spectrum of (A) malachite green-PVC film under N_2 atmosphere and (B) under 350 ppb HZ in N_2 . (C) and (D) are controls for a pure PVC film under N_2 and 350 ppb HZ, respectively.

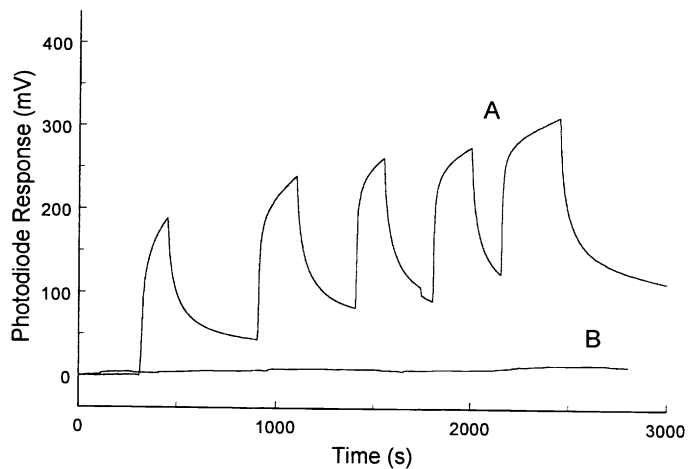


Figure 6. Raw responses to 5.4 ppm HZ for (A) PVC-MG sensor and (B) PVC film without MG.

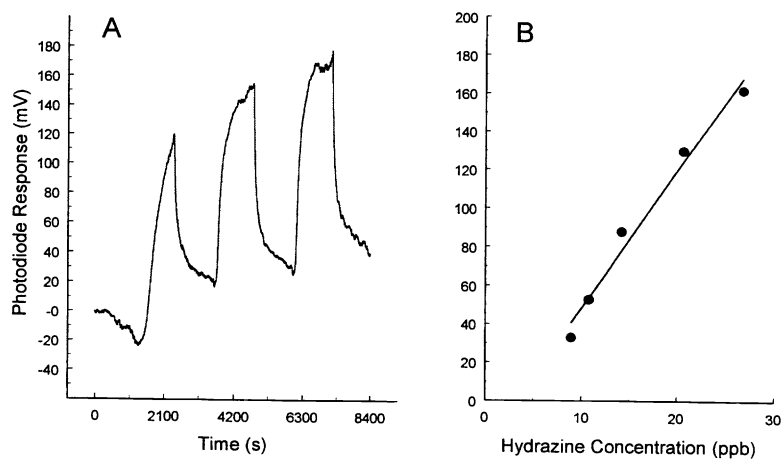


Figure 7. (A) raw response to 10 ppb HZ and (B) low-level concentration dependence of the sensor response.

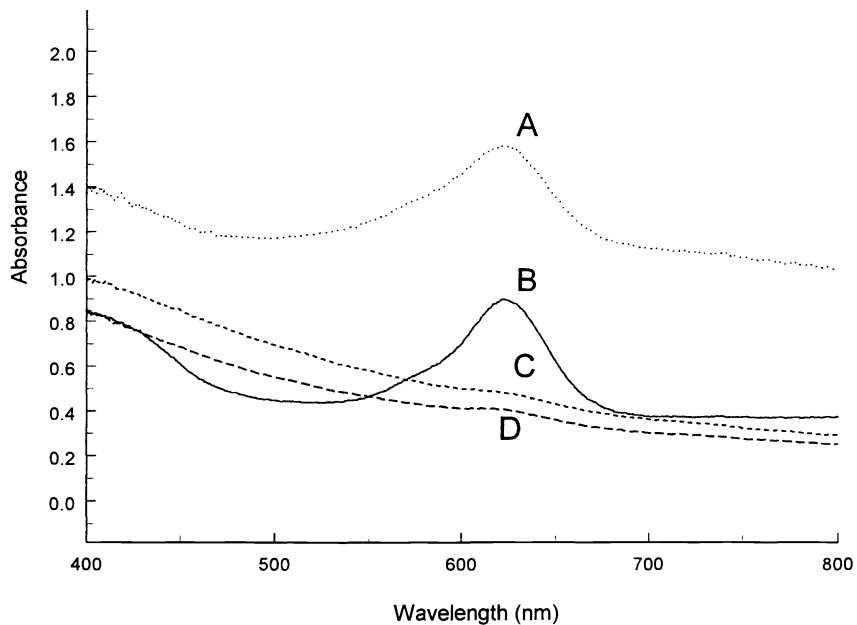


Figure 8. Effect of water vapor on transmission properties of the sensor. (A) and (C) are on-fiber spectra of PVC-MG and PVC, respectively, in the presence of water-saturated nitrogen. (B) and (D) are spectra of PVC-MG and PVC in the presence of dry nitrogen.

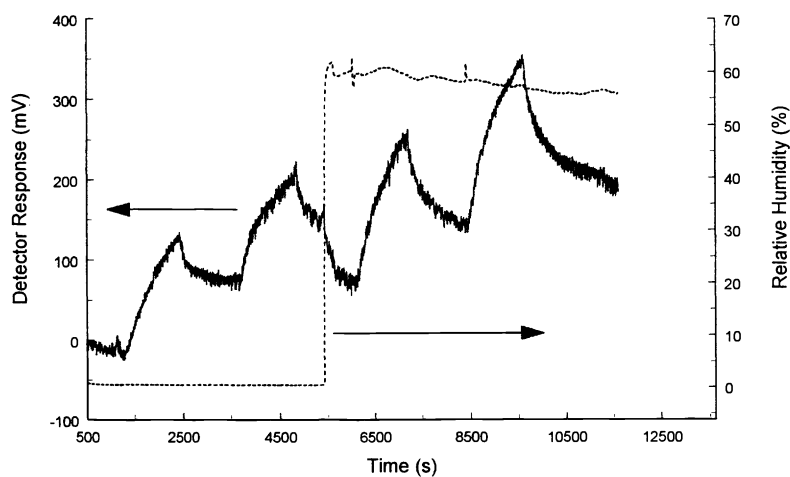


Figure 9. Response to 5.4 ppb HZ spanning a relative humidity step from 0% to 64 %.

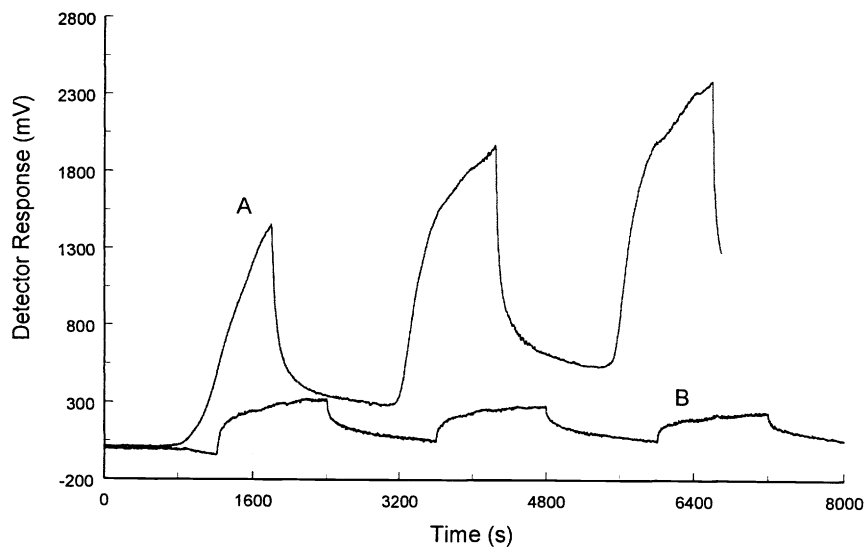


Figure 10. Sensor responses to (A) 62 ppb HZ and (B) 66 ppb NH₃.